Temperature-induced structure instability and magnetism of Fe/Cu(100)

D. Qian
Surface Physics Laboratory, Fudan University, Shanghai 200433, China
and Max-Planck-Institut för Mikrostrukturphysik, Weinberg 2, D-06120 Halle/Saale, Germany

X.F. Jin*
Surface Physics Laboratory, Fudan University, Shanghai 200433, China
and International Center for Quantum Structures, CAS, Beijing 100080, China

J. Barthel, M. Klaua, and J. Kirschner
Max-Planck-Institut för Mikrostrukturphysik, Weinberg 2, D-06120 Halle/Saale, Germany
(Received 28 February 2002; published 15 November 2002)

The structure and magnetism of epitaxially grown Fe films on Cu(100) at 300 K have been investigated *in situ* using high energy electron diffraction, low energy electron diffraction, scanning tunneling microscopy, and the magneto-optical Kerr effect. Based on a careful thickness calibration, the three well-known regions with distinct magnetic properties are determined accurately for Fe films on Cu(100). We claim that the traditional region II should be further divided into two parts II(1) and II(2), where the former remains region II in the traditional sense but the latter is a transition region between regions II and III. A theoretically predicted temperature driven Martensitic phase transition from face-centered-cubic (fcc) Fe to body-centered-cubic Fe is indeed realized in the transition region II(2).

DOI: 10.1103/PhysRevB.66.172406 PACS number(s): 75.50.Bb

The correlation between the structure and magnetism of a magnetic material remains an exciting subject in modern magnetism research. Presumably Fe has attracted the most attention, as it provides some unique features in this respect. In its thermodynamically stable phase Fe is a prototype ferromagnet with a bcc structure. However, the fcc phase of Fe is predicted to be nonmagnetic, ferromagnetic, antiferromagnetic, or of a spin-density wave character, depending strongly on the lattice constant.[1–9] Experimentally, it is known that bulk fcc Fe exists only at temperatures above 910 °C. However, the low temperature phase can be obtained as small particles ($\sim$50 nm) in a Cu matrix, and its magnetic structure has been determined to be a spin-density wave (SDW).[10,11]

On the other hand, the low temperature phase of fcc Fe can also be achieved by epitaxial growth on a Cu(100) substrate. As a function of film thickness, three stages with distinct magnetic properties have been observed for thermally deposited Fe films at 250–300 K (Refs. 12–21): (i) Films up to 3–4 ML (region I) have a body-centered-cubic (bcc) like structure[22] and are ferromagnetic with perpendicular magnetization. (ii) Films from 4 to 5 ML to 10 to 12 ML (region II) consist of a fcc antiferromagnetic part covered by some ferromagnetic surface layers with extended interlayer distance. (iii) Films thicker than 10–12 ML (region III) are bcc and ferromagnetic with in-plane magnetization.

The fcc-Fe/Cu(100) systems prepared at room temperature do not show any magnetic ordering at room temperature; they have to be cooled below 70 K to exhibit the complete magnetic behavior.[19,23] Therefore, the temperature induced structure instability during cooling and warming processes with reasonable fast or slow rates is indeed an important issue in order to obtain reproducible and solid experimental data. From our point of view this was mostly ignored in previous investigations, although it was theoretically predicted[25] and first noticed in experiment by Wuttig *et al.*[15]

In a previous work,[23] we focused mainly on the magnetic structure of region II and reached the conclusion that the antiferromagnetic part forms actually a spin-density wave. Here we address a couple of other issues about the structure and magnetism of Fe/Cu(100), which are also important in order to obtain a complete understanding of this long standing problem: (1) Experimentally the total magnetic moment versus film thickness curve was obtained by several groups,[17,19,21] but a definite conclusion about where to divide the three regions is still lacking, which would be needed to build a correct theoretical model. (2) It is well known that a Martensitic phase transition from fcc Fe to bcc Fe takes place at the borderline of regions II and III, and depends strongly on the growth temperature. A magnetic phase diagram with respect to the growth temperature and thickness was given by Li *et al.*, indicating that the transition occurs at thinner thickness if growing at lower temperatures, and vice verse.[19] However, it has not yet been systematically studied whether there exists a critical thickness for the thermally grown Fe films on Cu(100) at 250–300 K, such that the Martensitic phase transition can be just driven by cooling down from the growth temperature.

In this work, the film thickness of Fe on Cu(100) was cross checked by a quartz crystal microbalance, by reflection high energy electron diffraction (RHEED) intensity oscillations, and by a scanning tunneling microscopy (STM) with an accuracy within 0.1 ML.[23,27] We should emphasize here that the combination of STM and RHEED is crucial, while previous work used either the former or the latter but not both. The evolution of the Martensitic phase transition is monitored by its fingerprint in the corresponding STM images.[26] With these powerful experimental capabilities,

 ©2002 The American Physical Society

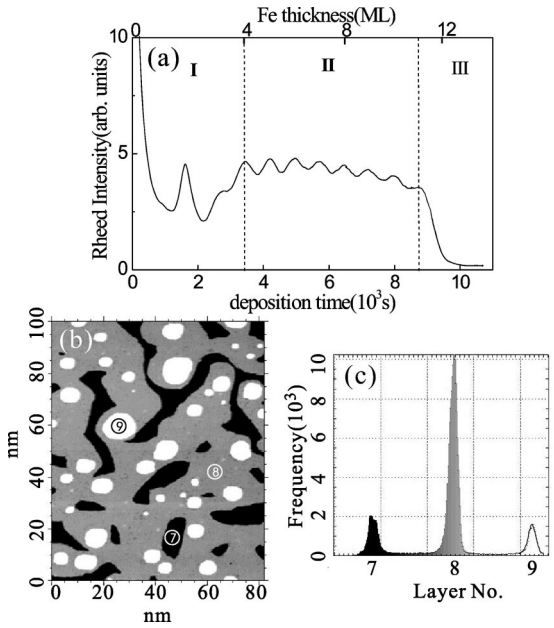

FIG. 1. (a) RHEED oscillations for Fe/Cu(100) grown at 300 K, (b) and (c) STM image for 8-ML Fe on Cu(100) and its histogram; 7, 8, and 9 indicate the layer number of Fe.

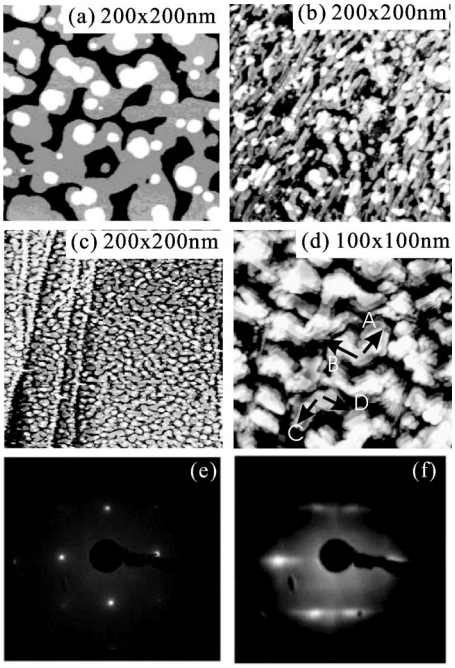

FIG. 2. STM images for (a) and (b) 9-ML Fe/cu(100) before and after cooling-warming procedure, (c) 10ML Fe/Cu(100) as grown. (d) 12-ML bcc Fe/Cu(100); *A*, *B*, *C*, and *D* indicate four domains of Fe(110) on Cu(100) (e), and (f) LEED patterns for 9-ML Fe/Cu(100) before and after the cooling-warming procedure ($E = 135$ eV).

both the temperature driven Martensitic phase transition and the total magnetic moment versus the film thickness curve can be determined accurately. The results show that the borderline between the regions I and II is at ~ 4 ML, and the borderline between regions II and III in the traditional sense is at ~ 11 ML, but the films between 9 and 11 ML in region II are unstable against cooling, and therefore belong to the new region II(2). Meanwhile, the films between 4 and 9 ML remain region II, in the traditional sense, and are now called region II(2). The temperature driven Martensitic phase transition occurs at a critical thickness of 9 ML for thermally deposited Fe films on Cu(100) at 300 K.

The experiment was carried out in a multifunctional ultrahigh vacuum system, equipped with RHEED, STM, low energy electron diffraction (LEED), cylindrical mirror analyzer based Auger electron spectroscopy (AES), and magneto-optical Kerr effect (MOKE) measurements. Prior to Fe deposition, the clean Cu(100) surface was prepared by cycles of 2-keV and 1-keV argon-ion bombardment at 300 K until no contaminations were detectable by AES, followed by annealing at 873 K for 15 min. This cleaning procedure was repeated until a sharp 1×1 LEED pattern was observed, and large atomically flat terraces were seen in STM. The base pressure was 8×10^{-12} mbar in the growth chamber, and it was better than 3×10^{-11} mbar during the Fe evaporation. Controlled by the quartz crystal microbalance and the RHEED intensity oscillations, the Fe deposition was stopped at the desired film thickness. However, the final thickness determination was done using STM after film deposition.[27]

Figure 1(a) shows a typical RHEED intensity oscillation curve as a function of film thickness, for the thermally deposited Fe on Cu(100) at 300 K. The first peak corresponds to the second layer of Fe, as reported earlier.[17,23] After four monolayers, Fe grows in a layer-by-layer mode. When the film is thicker than 11 ML, the oscillations disappear due to the complete fcc to bcc Fe phase transition. Figure 1(b) shows a typical STM image for 8-ML Fe on Cu(100). The number of 8 ML is obtained from the corresponding histogram of Fig. 1(c), from which it can be seen that the exposed surface area consists of about 80% of the eighth layer, 10% of the seventh layer, and 10% of the ninth layer, i.e., about 90% of the eighth layer is filled, while the missing 10% of this ML goes to the ninth layer. Each film thickness discussed in the following has been determined this way.

According to previous studies, it is known that a Martensitic phase transition from fcc Fe to bcc Fe takes place at about 10–12 ML, at a 250–300-K deposition temperature.[17] We studied this question based on the accurate film thickness calibration. It was demonstrated that STM is a very sensitive and powerful technique to detect the phase transition between fcc and bcc by observing the surface morphology as a fingerprint of the transition.[24,26] Using this STM fingerprint, it is then determined that Fe films below 9 ML are pure fcc Fe without any needles or ridges observable in the STM images, and are stable against cooling down to 70 K. Figure 1(b) is a representative STM picture for this region. The STM image for the 9-ML (as-grown) Fe film shows no detectable traces of needles seen in Fig. 2(a), similar to that of Fig. 1(b). However the film is unstable against cooling. Figure 2(b) shows a STM picture after the sample was cooled down to 70 K and warmed up to 300 K. There the ridgelike morphology can be clearly seen. It is found that the STM image for 10-ML (as-grown) Fe films already shows some needlelike morphology, as shown in Fig. 2(c) and it is un-

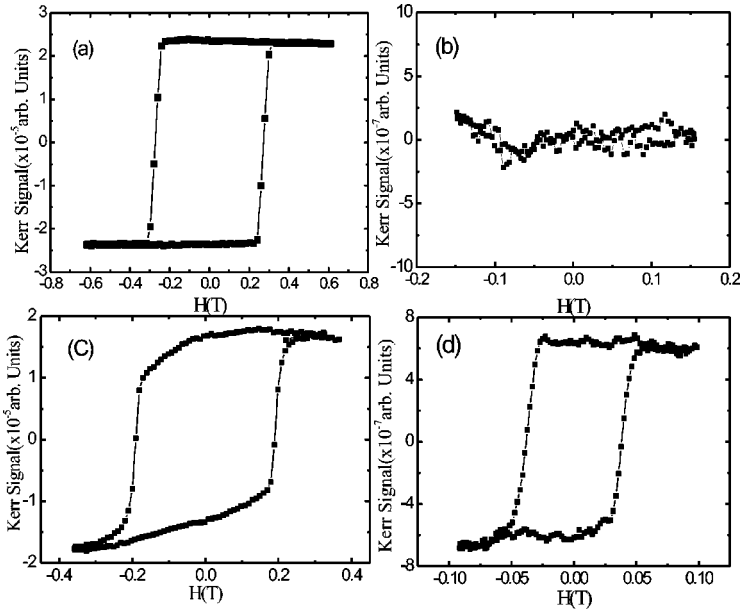

FIG. 3. (a) and (b) are the polar and longitudinal loops, respectively, for 9-ML Fe/Cu(100) measured at 70 K, (c) and (d) are the polar and longitudinal loops, respectively, after the system is warmed up to 190 K.

stable against cooling as well. Qualitatively speaking, Fe films with a thickness of 9 ML$\leqslant d \leqslant$11 ML have a similar property, i.e., an almost fcc-like morphology before cooling but a bcc-like morphology after cooling. For Fe (as-grown) films thicker than 11 ML, it is found that the STM images show a clear bcc-like morphology, as shown in Fig. 2(d) for a 12-ML Fe case. Films of 8 and 8.5 ML were found to be stable against cooling.

A profound difference is realized in the experiment between the temperature driven and film thickness driven Martensitic phase transitions. Figures 2(e) and 2(f) show the LEED patterns for 9-ML Fe on Cu(100) before and after the phase transition. Unlike the thick bcc Fe films on Cu(100) (the film thickness driven case), where the four $\langle 10 \rangle$ diffraction spots are split isotropically to form the quasi "3×1" structure,[15] Fig. 2(f) shows a highly anisotropic splitting. We checked the LEED *e*-beam at different points on the sample and obtained the same result. It is known from previous studies[15,28] that there should exist four domains along two directions in the former case, which can be actually seen in our STM image of Fig. 2(d) marked *A*, *B*, *C*, and *D*. Phenomenologically, the anisotropic splitting observed in the LEED pattern is also reflected in the corresponding STM image of Fig. 2(b). However, the mechanism behind is not trivial, and should be worked out in the future.

It should be mentioned that the 9-ML Fe film really lies at the border line. We observed in the experiment that the phase transition did not occur when the sample was quenched down to 70 K, but occurred when the sample was warmed up to 300 K. Due to the fact that our scanning tunneling microscope works only at room temperature, we try to prove this argument based on temperature dependent magnetism measurements. We show in Figs. 3(a) and 3(b), by measuring both the polar and longitudinal MOKE loops at 70 K, that the magnetic moment stays perpendicular to the plane during cooling. The squarelike polar MOKE loop in Fig. 3(a) clearly indicates that the magnetization is perpendicular to the surface at 70 K. However, it is found that the magnetic moment tends to lie down in the plane irreversibly during the warming up to 300 K. Figures 3(c) and 3(d) show the corresponding polar and longitudinal MOKE loops at 190 K, after the irreversible process has taken place. As a result of coexisting bcc and fcc Fe phases, the magnetization is no longer perpendicular to the surface, since the longitudinal MOKE loop looks more squarelike with a smaller coercivity. Nevertheless, it is also observed that the phase transition did take place during the cooling down process when the sample was slowly cooled down to 70 K.

It is interesting to compare the present results with those observed by Li *et al.*[19] In their work, it was found, depending on the growth temperatures, that region II can exhibit very different magnetic properties. When the growth temperature is above 250 K [region II(a)], the surface is ferromagnetic while the underlayers are antiferromagnetic. When the growth temperature is below 250 K [region II(b)], the film are ferromagnetic with in-plane easy axes. However, in the present work, we clearly demonstrate that films grown at 300 K, then cooled to low temperature, behave very differently in magnetism compare to those grown at low temperature. It is observed that films both of regions II(1) and II(2) grown at 300 K show the same magnetic property as that of region II(a) in Ref. 19, but region II(1) maintains the same magnetic property after cooling down to low temperature, while region II(2) changes its magnetic property. Therefore, it can be concluded that regions II(1) and II(2) are different from regions II(a) and II(b) in the previous work.

Based on the accurate thickness calibration, the polar Kerr signal at remanence for the 300-K grown Fe films on Cu(100) as a function of film thickness is measured at 70 K, as shown in Fig. 4. First of all, it is seen in the figure that the signal increases linearly in region I ($0<d\leqslant4$ ML). However, for Fe films thinner than 1 ML, the remanences of polar MOKE loops measured at 53 K are always small, as seen in the inset for a 1-ML Fe/Cu(100) loop. A similar result was also obtained at 30 K using a spin-resolved photoemission experiment.[29] Presumably Fe films thinner than 1 ML show

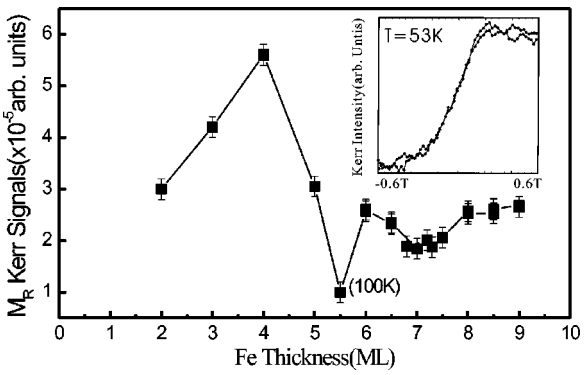

FIG. 4. The polar MOKE as a function of the Fe film thickness measured at 70 K.

squarelike loops below 30 K. Second, in subregion II(1) (4–9 ML) it is found that the signal decreases as the film is thicker than 4 ML and reaches a minimum at 5.5 ML, then oscillates up to 9 ML. Because the coercivity of the MOKE loop taken at 70 K, at the particular thickness of 5.5 ML, exceeds the maximum magnetic field ($\sim$8000 Oe) available in our setup, in this figure we show data measured at 100 K instead. According to Berger *et al.*,[13] this anomaly of the coercivity is caused by a magnetic frustration in the mixed phase of bcc-like and fcc Fe structures. Third, we discussed above that there exists another subregion II(2) with an Fe thickness $9 < d \leqslant 11$ ML where the fcc Fe films are still stable at 300 K but become unstable during cooling. They do not appear in the curve because all the data shown in this figure were polar MOKE data taken at 70 K. Finally, in the region III $d > 11$ ML, the films of Fe/Cu(100) become bcc, with the magnetic magnetization lying in the plane.

Finally, we try to go a step further based on the data presented in Fig. 4, while keeping in mind that the conclusion has to be verified by further direct measurements. According to our previous work[23] the difference (0.9×10^{-5} arb. units according to Fig. 4) of MOKE signals at 7 and 6 ML corresponds to about one layer of the SDW that is aligned parallel to the ferromagnetic surface layers. If we assume that the MOKE signal measured in Fig. 4 is proportional to the total magnetic moment of this system along the surface normal direction, while the ferromagnetic phase is in a high spin state and has the same magnetic moment in regions I and II, then we can estimate from Fig. 4 that the total magnetic moment of the ferromagnetic phase at 4 ML corresponds to a MOKE signal of 5.6×10^{-5} arb. units, i.e., the signal for a single ferromagnetic layer is about 1.4×10^{-5} arb. units. This leads to our conclusion that the magnetic moment per atom in the spin density wave is about 60% of that of the ferromagnetic phase.

D.Q. and X.F.J acknowledge the support from MPI Halle during their stay in Halle. X.F.J. also acknowledges the partial support from the National Natural Science Foundation of China, the Cheung Kong Program, the Hong Kong Qiushi Science Foundation, the Y.D. Fok Education Foundation, and Shanghai Science and Technology Committee.

*Corresponding author. Email address: xfjin@fudan.ac.cn; FAX: 86-21-65104949.

[1] C.S. Wang, B.M. Klein, and H. Krakauer, Phys. Rev. Lett. **54**, 1852 (1985).
[2] F.J. Pinski *et al.*, Phys. Rev. Lett. **56**, 2096 (1986).
[3] V.L. Moruzzi *et al.*, Phys. Rev. B **34**, 1784 (1986).
[4] O.N. Mryasov, V.A. Gubanov, and A.I. Liechtenstein, Phys. Rev. B **45**, 12330 (1992).
[5] M. Uhl, L.M. Sandratskii, and J. Kubler, Phys. Rev. B **50**, 291 (1994).
[6] M. Koerling and J. Ergon, Phys. Rev. B **54**, R8293 (1996).
[7] Y.M. Zhou, D.S. Wang, and Y. Kawazoe, Phys. Rev. B **59**, 8387 (1999).
[8] K. Knopfle, L.M. Sandratskii, and J. Kubler, Phys. Rev. B **62**, 5564 (2000).
[9] R. Lorenz and J. Hafner, Phys. Rev. B **58**, 5197 (1998).
[10] Y. Tsunoda, J. Phys. C **1**, 10427 (1989).
[11] Y. Tsunoda, Y. Nishioka, and R.M. Nicklow, J. Magn. Magn. Mater. **128**, 133 (1993).
[12] R.E. Camley and D.Q. Li, Phys. Rev. Lett. **84**, 4709 (2000).
[13] A. Berger *et al.*, J. Magn. Magn. Mater. **183**, 35 (1998).
[14] K. Kalki *et al.*, Phys. Rev. B **48**, 18344 (1993).
[15] M. Wuttig *et al.*, Surf. Sci. **291**, 14 (1993).
[16] H. Zillgen, B. Feldmann, and M. Wuttig, Surf. Sci. **321**, 32 (1994).
[17] J. Thomassen *et al.*, Phys. Rev. Lett. **69**, 3831 (1992); M. Wuttig and J. Thomassen, Surf. Sci. **282**, 237 (1993).
[18] W. Keune *et al.*, Physica B **161**, 269 (1989).
[19] D. Li *et al.*, J. Appl. Phys. **76**, 6425 (1994); Phys. Rev. Lett. **72**, 3112 (1994).
[20] S. Muller *et al.*, Phys. Rev. Lett. **74**, 765 (1995).
[21] R. Vollmer and J. Kirschner, Phys. Rev. B **61**, 4146 (2000).
[22] Albert Biedermann *et al.*, Phys. Rev. Lett. **87**, 086103 (2001).
[23] D. Qian *et al.*, Phys. Rev. Lett. **87**, 227204 (2001).
[24] Albert Biedermann, Michael Schmid, and Peter Varga, Phys. Rev. Lett. **86**, 464 (2001).
[25] K. Kadau and P. Entel, J. Magn. Magn. Mater. **198-199**, 531 (1993).
[26] J. Shen *et al.*, Surf. Sci. **407**, 90 (1998).
[27] X.F. Jin *et al.*, Phys. Rev. B **60**, 11809 (1999).
[28] F. Scheurer *et al.*, Phys. Rev. B **48**, 9890 (1993).
[29] D. Pescia *et al.*, Phys. Rev. Lett. **58**, 2126 (1987).